(4)

AFGL-TR-86-0219

Borehole Tilt Results From Charlevoix, Quebec

John Peters
Jochen Kumpel
Christopher Beaumont

Dalhousie University
Oceanography Department
Halifax, Nova Scotia
CANADA

23 April 1987

Scientific Report No. 2

AIR FORCE GEOPHYSICS LABORATORY
AIR FORCE SYSTEMS COMMAND
UNITED STATES AIR FORCE
HANSCOM AIR FORCE BASE, MASSACHUSETTS 01731-5000

Unclassified

SECURITY CLASSIFICATION OF THIS PAGE

REPORT DOCUMENTATION PAGE

1a. REPORT SECURITY CLASSIFICATION Unclassified	1b. RESTRICTIVE MARKINGS
2a. SECURITY CLASSIFICATION AUTHORITY	3. DISTRIBUTION/AVAILABILITY OF REPORT Approved for public release; Distribution unlimited
2b. DECLASSIFICATION/DOWNGRADING SCHEDULE	
4. PERFORMING ORGANIZATION REPORT NUMBER(S)	5. MONITORING ORGANIZATION REPORT NUMBER(S) AFGL-TR-86-0219
6a. NAME OF PERFORMING ORGANIZATION Dalhousie University Oceanography Department 6b. OFFICE SYMBOL (If applicable)	7a. NAME OF MONITORING ORGANIZATION Air Force Geophysics Laboratory
6c. ADDRESS (City, State and ZIP Code) Halifax, Nova Scotia, CANADA	7b. ADDRESS (City, State and ZIP Code) Hanscom AFB Massachusetts 01731
8a. NAME OF FUNDING/SPONSORING ORGANIZATION 8b. OFFICE SYMBOL (If applicable)	9. PROCUREMENT INSTRUMENT IDENTIFICATION NUMBER F19628-83-K-0023
8c. ADDRESS (City, State and ZIP Code)	10. SOURCE OF FUNDING NOS. PROGRAM ELEMENT NO.: 61102F; PROJECT NO.: 2309; TASK NO.: G2; WORK UNIT NO.: AN
11. TITLE (Include Security Classification) Borehole Tilt Results From Charlevoix, Quebec	
12. PERSONAL AUTHOR(S) John Peters, Jochen Kumpel*, Christopher Beaumont	
13a. TYPE OF REPORT Scientific Report #2 13b. TIME COVERED FROM _____ TO _____	14. DATE OF REPORT (Yr., Mo., Day) 23 April 1987 15. PAGE COUNT 26
16 SUPPLEMENTARY NOTATION (Refer to Final Report - AFGL-TR-87-0134; ADA201039) * Geophysics Institute, Kiel University, Kiel, West Germany	
17. COSATI CODES FIELD / GROUP / SUB. GR.	18. SUBJECT TERMS (Continue on reverse if necessary and identify by block number) Earth Tides Tilt Meters Earthquake Prediction

19. ABSTRACT (Continue on reverse if necessary and identify by block number)

Results from the analysis of recordings from the Charlevoix borehole tilt experiment are presented and discussed. Time variations in the tilt tidal admittance are shown to be related to the time variations in the marine loading from the nearby St. Lawrence estuary. Most of the variability in the sub-tidal tilts is associated with groundwater fluctuations at the Charlevoix site, the residual drift rates varying between 0.01 and 1.0 μrad/yr depending on the tiltmeter. The detectability of coherent regional signals is 2 μrad/yr in the south direction and 0.25 μrad/yr in the east.

20. DISTRIBUTION/AVAILABILITY OF ABSTRACT UNCLASSIFIED/UNLIMITED ☐ SAME AS RPT. ☐ DTIC USERS ☐	21. ABSTRACT SECURITY CLASSIFICATION Unclassified
22a. NAME OF RESPONSIBLE INDIVIDUAL John J. Cipar	22b TELEPHONE NUMBER (Include Area Code) 22c OFFICE SYMBOL AFGL/LWH

DD FORM 1473, 83 APR EDITION OF 1 JAN 73 IS OBSOLETE.

Unclassified

SECURITY CLASSIFICATION OF THIS PAGE

TABLE OF CONTENTS

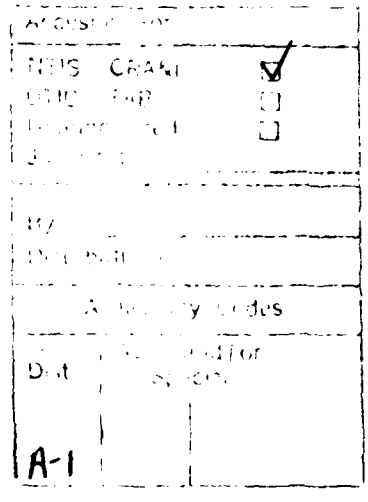

INTRODUCTION

An array of three borehole tiltmeters has been established in the seismically active Charlevoix region of Québec. The measurements are designed to sample the earth tide response as a possible indicator of changing crustal conditions and, by monitoring secular and transient tilts, to directly detect regional crustal deformations associated with processes occurring at depth.

In this report we discuss the status of the experimental program and the results from analysis of the tides, the secular component and the non-linear tidal harmonics, or overtides. Time variations of the tilt tidal admittance have been studied in conjunction with parallel analyses of data from nearby tide gauges. We show that most of the variability in the tilt is reflected in the marine tide. A similar analysis of continuous tide gauge data recorded at stations distributed over the whole of the St. Lawrence estuary during 1972 to 1974 was analysed as a step towards establishing a spatial characterization of the marine tide variability. Results of regression analysis of the sub-tidal tilts with continuous water level measurements confirm that for all three boreholes most of the variance is associated with hydrological processes and that these effects are attenuated with depth. The mean admittance results for the non-linear constituents M_4 and M_6 are in good agreement with estimates based on a loading model for the St. Lawrence estuary.

EXPERIMENTAL DETAILS

The array consists of three boreholes forming a triangle of approximately 80m side. Two of the holes, 1 and 2, are 47m deep and the third, borehole 3, is 100m deep (Peters and Beaumont, 1985). The holes are instrumented with Bodenseewerk Gbp 10 borehole pendulums and the data are continuously recorded on strip chart recorders. Figure 1 shows the status of data collection and processing at the end of 1984. Since the end of 1982, the data have been virtually continuous (98.3%) for borehole 1, and totally continuous for boreholes 2 and 3.

While the azimuth of the two shallow instruments is determined optically (Peters and Beaumont, 1985) and is known to within 0.5 degrees, that of the third hole, in the absence of a line of sight, was estimated by a onetime gyroscopic survey. The survey result is, however, inconsistent with the observed tidal response, indicating that either the survey or the positioning of the tiltmeter in the hole is in error by about 60 degrees. The azimuth has been estimated on the basis of the observed tide but can only be determined to within plus or minus 10 degrees. This is not a hindrance to studies of the stability of the tidal admittance.

TIDAL ANALYSIS - THE LINEAR TIDE

A detailed account of the tidal analysis method is given in Peters and Beaumont (1985). That discussion includes a mathematical description and justification of the

HYCON program. The essence of the method lies in the recognition that real tidal data cannot in general be modelled as a sum of known astronomical frequencies superimposed on white noise. Additional deterministic components are inevitably present to some degree, and these will interact with the data window potentially to bias the tidal estimates. HYCON permits the use of the Hanning window which, when applied to the data, has the effect of reducing sidelobe leakage in the frequency domain from unmodelled spectral components. This is particularly important in time variant analysis where artificial modulations are difficult to distinguish from those due to physical sources.

Data from the tide gauges St. Joseph de la Rive (12 Km to the south of the site) and Tadoussac (90 Km north-east) recorded during 1983 were analysed in conjunction with the tilt from boreholes 1 and 2 for the same period. The results for M_2 are shown in figures 2 and 3 for amplitude and phase, respectively. The range of the tilt amplitude variations is around 10% and correlates very strongly among the four components. The correlation also extends strongly to the two tide gauge series and indicates a clear connection with the tilt through loading. However, the range of the variations at St. Joseph de la Rive, the nearest gauge, is fractionally only half that of the tilt. Since we expect the nearest tide gauge to be most representative of the loading, it remains for us to explain the "amplified" tilt response. The answer may be connected to the surprising phase characteristics shown in figure 3.

The four tilt components behave nearly identically for M_2 phase, again confirming a regional effect. The two tide gauges, though, not only show no correlation with the tilt, they do not correlate with one another. We investigated further this apparent lack of spatial coherency in the M_2 marine phase variations. During the period August, 1972 to July, 1974 all of the permanent tide gauges in St. Lawrence estuary (shown in figure 4) operated continuously. The data sets were analysed in the same way as those above. The results are plotted in figures 5 and 6 for the $P_1S_1K_1$ group amplitude and phase, and in figures 7 and 8 for M_2.

The diurnal constituents (here represented by $P_1S_1K_1$) show remarkable coherency over the whole estuary both in amplitude and phase. In contrast, the M_2 amplitudes (figure 7) are only weakly coherent on a regional scale, although in the vicinity of the Charlevoix area, a few gauges (4, 5 and 6) correlate well. The phases show no such systematic behaviour. It is possible that the rapid spatial change in the admittance patterns could account for 1) the differences between the tilt and the tide gauge phase variations and 2) the difference in the fractional changes in admittance amplitude between the tilt and the tide gauge at St. Joseph de la Rive. Clearly, estimating the variations in the loading admittance for M_2 cannot be done on the basis of a single tide gauge.

Since we have established that the variations in the tilt tidal admittance are connected with the loading input, to what extent can we correct for the input fluctuations and thereby study the stability of the Earth's tidal response? In figures 9 to 12, we have plotted on polar diagrams the O_1 south and east and M_2 south and east admittance functions for 1983. The light shaded area represents the range of the observations. The superimposed dark area is the area representing the range of the residual admittance tilt after regression on the tide gauge at St. Joseph de la Rive. In the case of O_1, since both the amplitudes and the phases, respectively, were highly correlated, each was modelled separately. Only

the amplitude could be modelled for M_2. The phase range of the M_2 residual therefore is the same as the observations. The filled circle in each plot represents the degree to which the redundant admittance determinations for each direction are incoherent (based on the range of the residual from the regression of 106 on 107). This places a lower limit on the detectability of regional signals around 10% or 0_1 and 1% to 2% for M_2. Note that in the four cases there is little room for improvement (in terms of amplitude) of the model of the time varying loading input.

SUB-TIDAL TILTS

Figure 13 is a plot of the low pass filtered observations from the tiltmeters in boreholes 1, 2 and 3 and water level from well b(70) adjacent to borehole 2 (lower part); and the residual from the linear regression of the water level on the tilt (top part). The long term tilt fluctuations are similar in size and character for the borehole 1 and 2 (47m deep) components. They range between 2 and 4 μrad and correlate with water level. In borehole 3 the X-component, with azimuth approximately 120 degrees, is dominated by an exponential term possibly due to instrumental instability arising from mechanical repairs. The y-component (azimuth 210 degrees) correlates strongly with the water level fluctuations. Table 1 shows the tilt/water level transfer coefficient for each component as well as an estimate of the linear drift (with 95% confidence limits) derived from least squares fitting of a straight line to each component residual. Estimates are not yet given for the X-component of hole 3.

The water level correlation persists in the residuals for both of the east components and hole 1 south, indicating that the regression model can be refined. For all components the drift rates are well determined. In the south, holes 1 and 2 drift in opposite directions at 1 μrad/yr, placing a lower limit on the detectability of tectonic tilts at 2 μrad/yr. The hole 1 east rate is negligible and may represent an upper limit to the regional trend. However, basing the detectability of tectonic signals on the level of incoherency between redundant measurements, the lowest detectable regional signal in the east direction is 0.25 μrad/yr. This is equivalent to the rates reported in the comparative tilt experiment at Pinon Flat, California which has measured among the lowest rates so far reported [Wyatt *et al.*, 1984].

The large difference between the observed drift rates emphasizes a major difficulty for borehole measurements. Although the effective measurement baseline in the Earth is much larger than the instrument baselength (because of the rigidity of the borehole casing), the coupling interval of the instrument to the casing is only 1.5m. The intrinsic stability of long baseline instruments like the 535m UCSD tiltmeter [Wyatt *et al.*, 1984] is potentially 300 times better. In boreholes, very high stability is as much a function of good luck as good management.

NON-LINEAR TIDES

Beaumont [1978] and Agnew [1981] have discussed possible sources of non-linearity in the Earth which may be manifest in the tidal response. Figure 14 shows the amplitude

spectra for boreholes 1 and 2 in the non-linear bands showing significant peaks. In table 2 we compare the observed mean M_4 and M_4 admittances with those predicted on the basis of a loading model of the St. Lawrence estuary. The model is the same as that of Peters and Beaumont (1985) using in this case the M_4 and M_6 tidal distribution. Although for these constituents the marine tide distribution is poorly known (because of its rapid spatial variability) there is good agreement, especially in the east direction, between theory and observation. This suggests that most of the non-linear content of the tilt is due the loading input.

SUMMARY AND CONCLUSIONS

Time variant tidal analysis of the continuous 1983 tilt data in conjunction with marine data from the St. Lawrence estuary has confirmed that variations in the tilt tidal admittance are largely due to the time varying loading input. Regression analysis of the tilt and tide gauge admittance series reduces the M_2 amplitude baseline for the detection of crustal response anomalies to the 1% to 2% level and for the 0_1 baseline, to the 10% level. The outstanding problem is to characterize the spatial distribution of the marine M_2 variations so that a correction for the variable loading input function can be made for both amplitude and phase.

The sub-tidal tilts correlate strongly with water table fluctuations. Regression analysis of the tilt and water level series indicates that a linear model explains most of the variance. The water level effect is attenuated with depth. However, since the response is strongly polarized (see Peters and Beaumont, 1985), we need to study the response for the three boreholes in the sensitive azimuth to determine the degree of attenuation. The linear drift rates of the tilt measurements are quite variable. Based on 1.5 years of data, the detectability of coherent regional signals is 2 μrad/yr in the south direction and 0.25 μrad/yr in the east.

There are prominent non-linear tidal components in the tilt observations. The best determined of these, M_4 and M_6, compare well with the amplitude and phase predicted by a loading model of the St. Lawrence estuary, indicating that there is no obvious non-linear crustal response anomaly detectable in the data.

REFERENCES

Agnew, D.C., Nonlinearity in rock: evidence from earth tides, J. Geophys. Res., *86*, 3969-39, 1981.

Beaumont, C., Linear and nonlinear interactions between the earth tide and a tectonically stressed earth, in: Applications of Geodesy to Geodynamics, I. Mueller, ed., Ohio State University Press, 299-318, 1978.

Peters, J., and C. Beaumont, Borehole Tilt Measurements from Charlevoix, Quebec, J. Geophys. Res. *90*, 12, 791-12, 806, 1985.

Wyatt, F., R. Bilham, J. Beavan, A.G. Sylvester, T. Owen, A. Harvey, C. Macdonald, D.D. Jackson, and D.C. Agnew, Comparing tiltmeters for crustal deformation measurement - a preliminary report, Geophys. Res. Letts, 11, no. 10, 963-966, 1984.

FIGURE CAPTIONS

Figure 1. Data available from the borehole tiltmeter experiment.

Figure 2. Plots versus time of the changes in M_2 amplitude for the south and east components of tilt in boreholes 1 and 2 and the tide gauges at St. Joseph de la Rive and Tadoussac. The percent scales represent fractions of the mean amplitude.

Figure 3. Plots versus time of the changes in M_2 phase lag for the south and east components of tilt in boreholes 1 and 2 and the tide gauges at St. Joseph de la Rive and Tadoussac. The percent scales represent fractions of the mean amplitude.

Figure 4. Map of the St. Lawrence estuary showing locations of tide gauges. The Charlevoix site overlaps STJ (6) on this scale.

Figure 5. Plots versus time of the changes in the $P_1S_1K_1$ group amplitudes for the tide gauges shown on the map in figure 4. The number to the right of each series corresponds with the tide gauge number in figure 4. The dotted curves trace out the error envelope for each time varying amplitude series based on the 95% residual error calculated in HYCON for each overlapping estimate. The time axis is in days relative to Julian day 1, 1972.

Figure 6. Plots versus time of the changes in the $P_1S_1K_1$ group phase lag for the St. Lawrence tide gauges. Details as in figure 5.

Figure 7. Plots versus time of the changes in the M_2 amplitudes for the St. Lawrence tide gauges. Details as in figure 5.

Figure 8. Plots versus time of the changes in the M_2 phase lags for the St. Lawrence tide gauges. Details as in figure 5.

Figure 9. Polar representation of the variability of the 1983 tilt data for O_1 in the south direction. Amplitude is proportional to the distance of the point from the origin. Relative amplitudes are scaled by the 10% scale interval. The solid line represents the mean admittance vector. G is Greenwich phase lag. Details of the computations are explained in the text.

Figure 10. Polar representation of the variability of the 1983 tilt data for O_1 in the east direction. Details as for figure 9.

Figure 11. Polar representation of the variability of the 1983 tilt data for M_2 in the south direction. Details as for figure 9.

Figure 12. Polar representation of the variability of the 1983 tilt data for M_2 in the east direction. Details as for figure 9.

Figure 13. Lower Panel. Plots versus time of water level and the low pass filtered tilt observations from boreholes 1 and 2. Upper Panel. Plots versus time of the residual from regression of the water level on the low pass filtered tilt observations. The curves are identified by the borehole number and the letter S(outh), E(ast), X or Y according to the component direction. The time axis is the same for both panels, marked in days relative to 27 Nov., 1981.

Figure 14. Fourier amplitude spectra of the non-linear tidal bands.

TABLE 1. COMPARISON OF SUB-TIDAL CHARACTERISTICS AMONG BOREHOLES

	Hole 1		Hole 2		Hole 3	
	South	East	South	East	X(120)	Y(210)
Transfer Coeff nrad/cm	2.35	1.21	2.46	5.02	-	0.78
Drift Rate μrad/yr	-0.97	0.01	1.01	0.26	-	0.04
Error (95%) μrad/yr	0.02	0.03	0.01	0.03	-	0.01

TABLE 2. COMPARISON OF M_4 AND M_4 - OBSERVED VERSUS THEORY

	SOUTH			EAST		
	Hole 1	Hole 2	Model	Hole 1	Hole 2	Model
M_4						
Amplitude nrad	2.19 (0.08)	3.08 (0.11)	3.74	6.80 (0.17)	7.77 (0.20)	6.66
G deg	340.2 (3.9)	339.5 (3.1)	339	352.7 (1.9)	352.9 (2.1)	346
M_6						
Amplitude nrad	0.34*	0.44*	0.91	1.58 (0.08)	1.87 (0.14)	1.72
G deg	100*	75*	63	25.4 (3.8)	22.8 (5.0)	23.5

*Preliminary estimate
*Bracketed figures are 95% error estimates

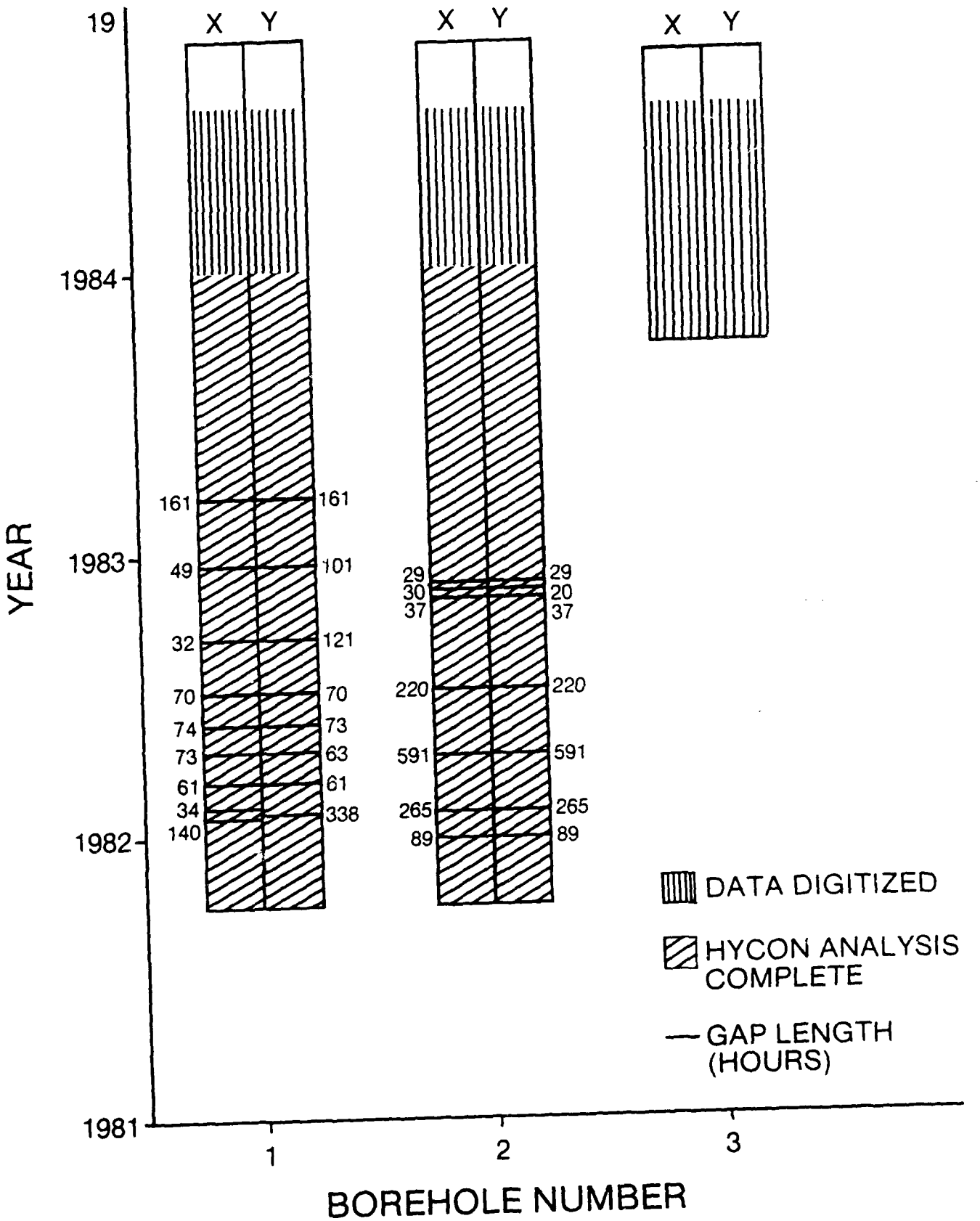
19
1984
1983
1982
1981
YEAR
X Y
X Y
X Y
161
161
49
101
32
121
70
70
74
73
73
63
61
61
34
338
140
29
29
30
20
37
37
220
220
591
591
265
265
89
89
DATA DIGITIZED
HYCON ANALYSIS COMPLETE
GAP LENGTH (HOURS)
1
2
3
BOREHOLE NUMBER

FIGURE 1

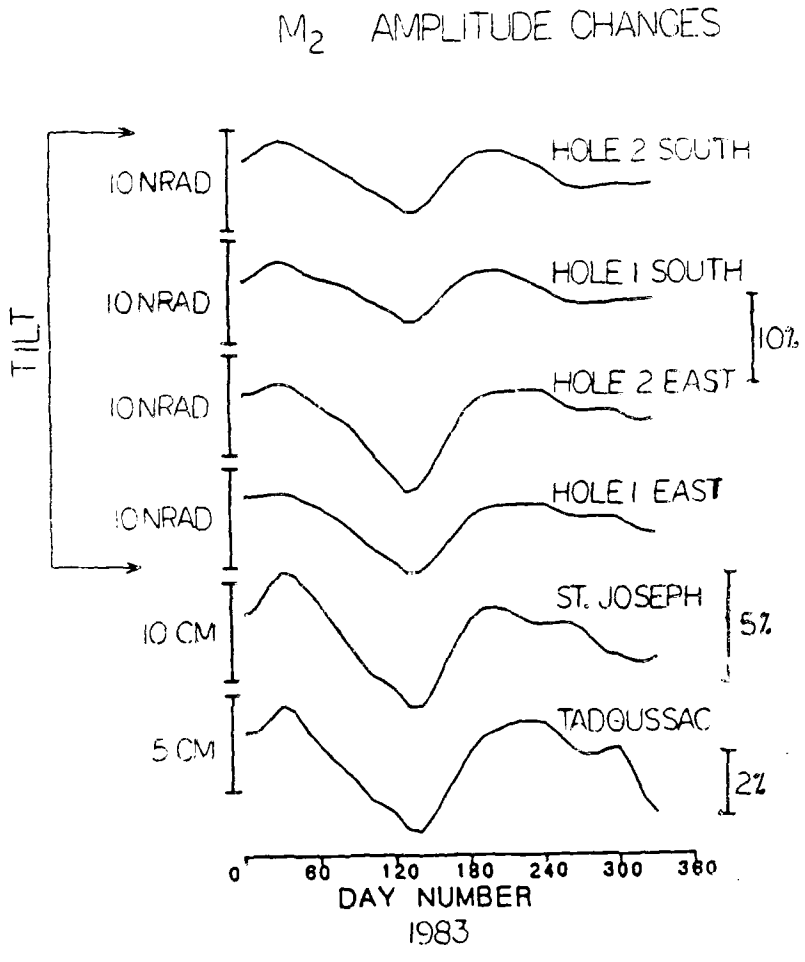

Figure 2 Plots versus time of the changes in M_2 amplitude for the south and east components of tilt in boreholes 1 and 2 and the tide gauges at St. Joseph de la Rive and Tadoussac. The percentage scales represent fractions of the mean amplitude.

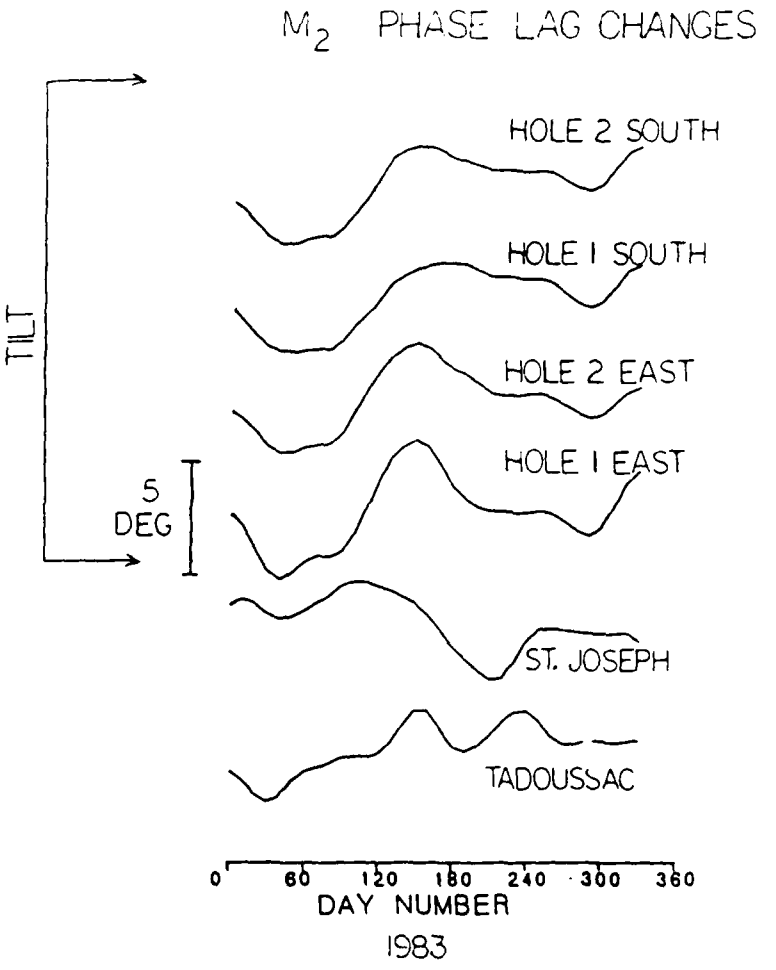

Figure 3 Plots versus time of the changes in M_2 phase lag for the south and east components of tilt in boreholes I and 2 and the tide gauges at St. Joseph de la Rive and Tadoussac.

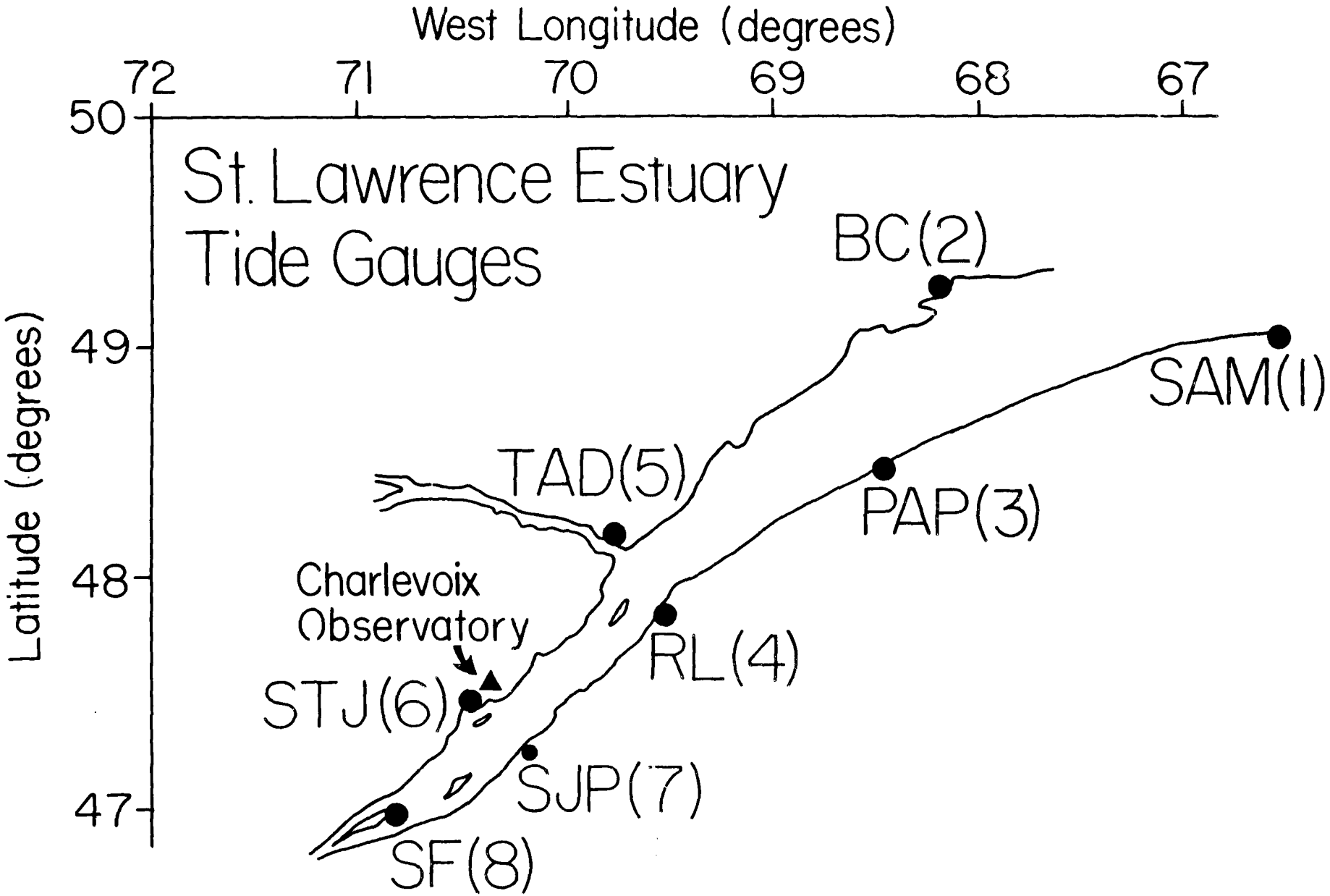
West Longitude (degrees)
72
71
70
69
68
67
50
49
48
47
Latitude (degrees)
St. Lawrence Estuary
Tide Gauges
BC(2)
SAM(1)
TAD(5)
PAP(3)
Charlevoix
Observatory
RL(4)
STJ(6)
SJP(7)
SF(8)

FIGURE 4

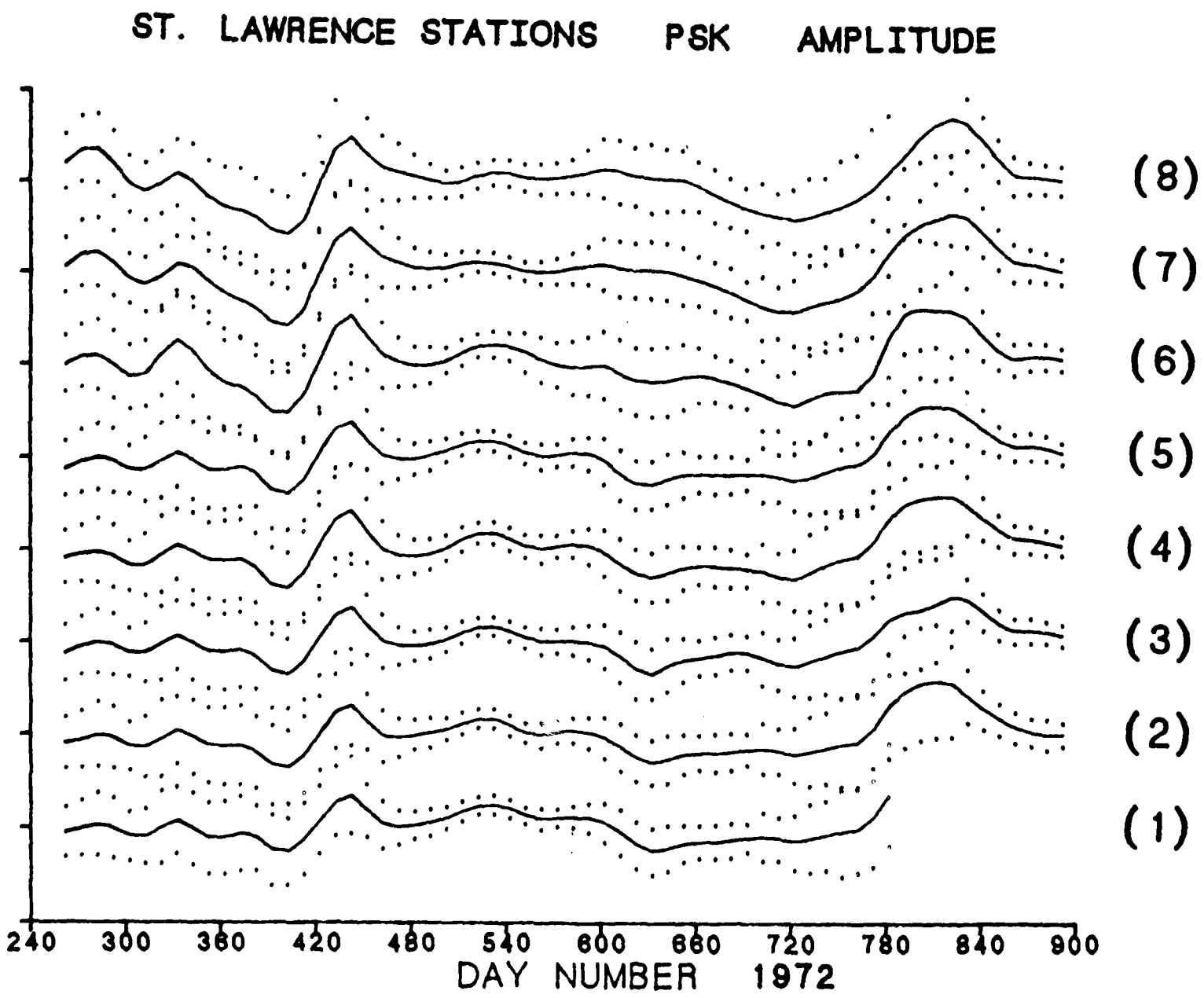
ST. LAWRENCE STATIONS PSK AMPLITUDE
1div=10cm
(8)
(7)
(6)
(5)
(4)
(3)
(2)
(1)
240
300
360
420
480
540
600
660
720
780
840
900
DAY NUMBER 1972

FIGURE 5
13

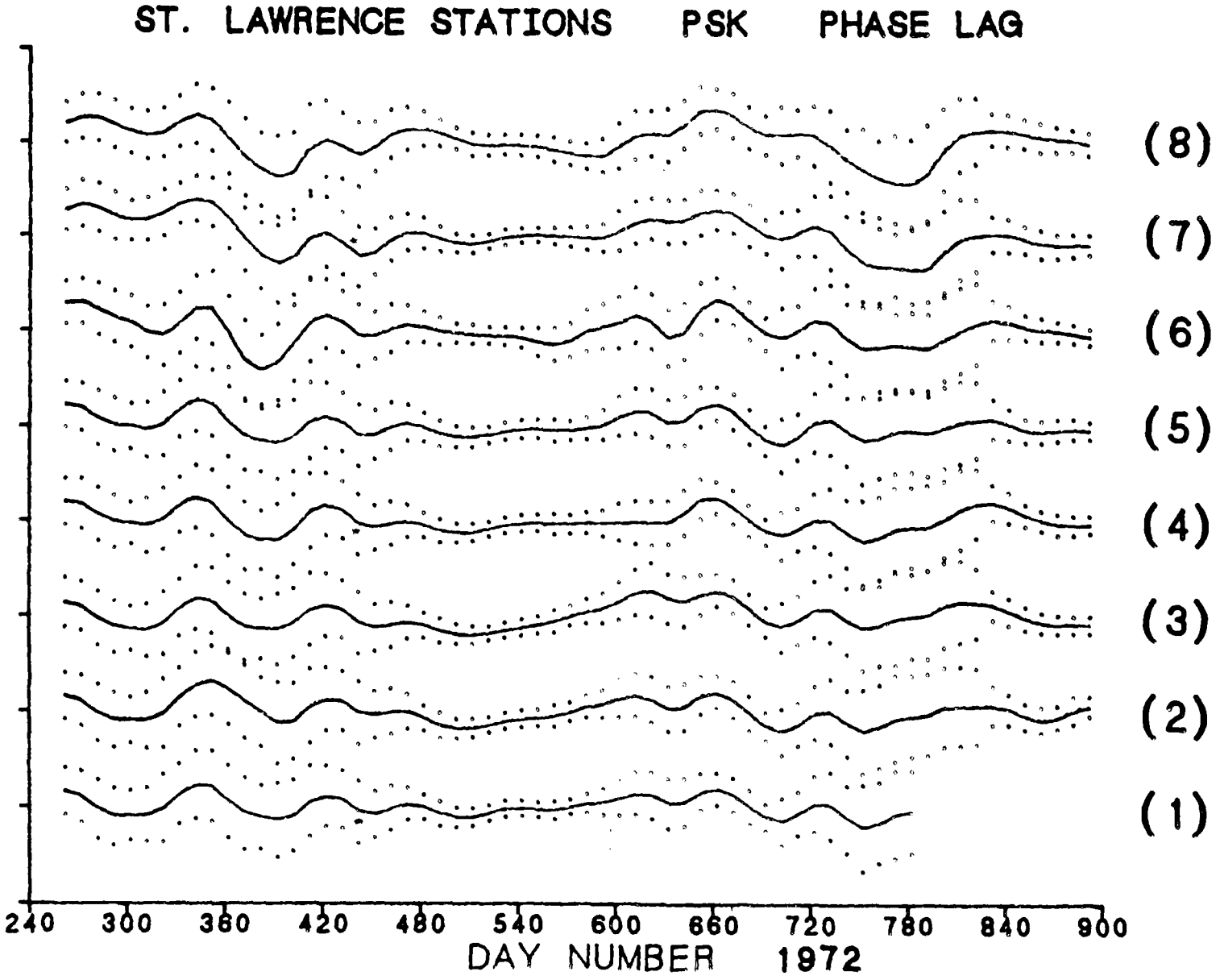
ST. LAWRENCE STATIONS PSK PHASE LAG
1div=30deg
(8)
(7)
(6)
(5)
(4)
(3)
(2)
(1)
240
300
360
420
480
540
600
660
720
780
840
900
DAY NUMBER 1972

FIGURE 6
14

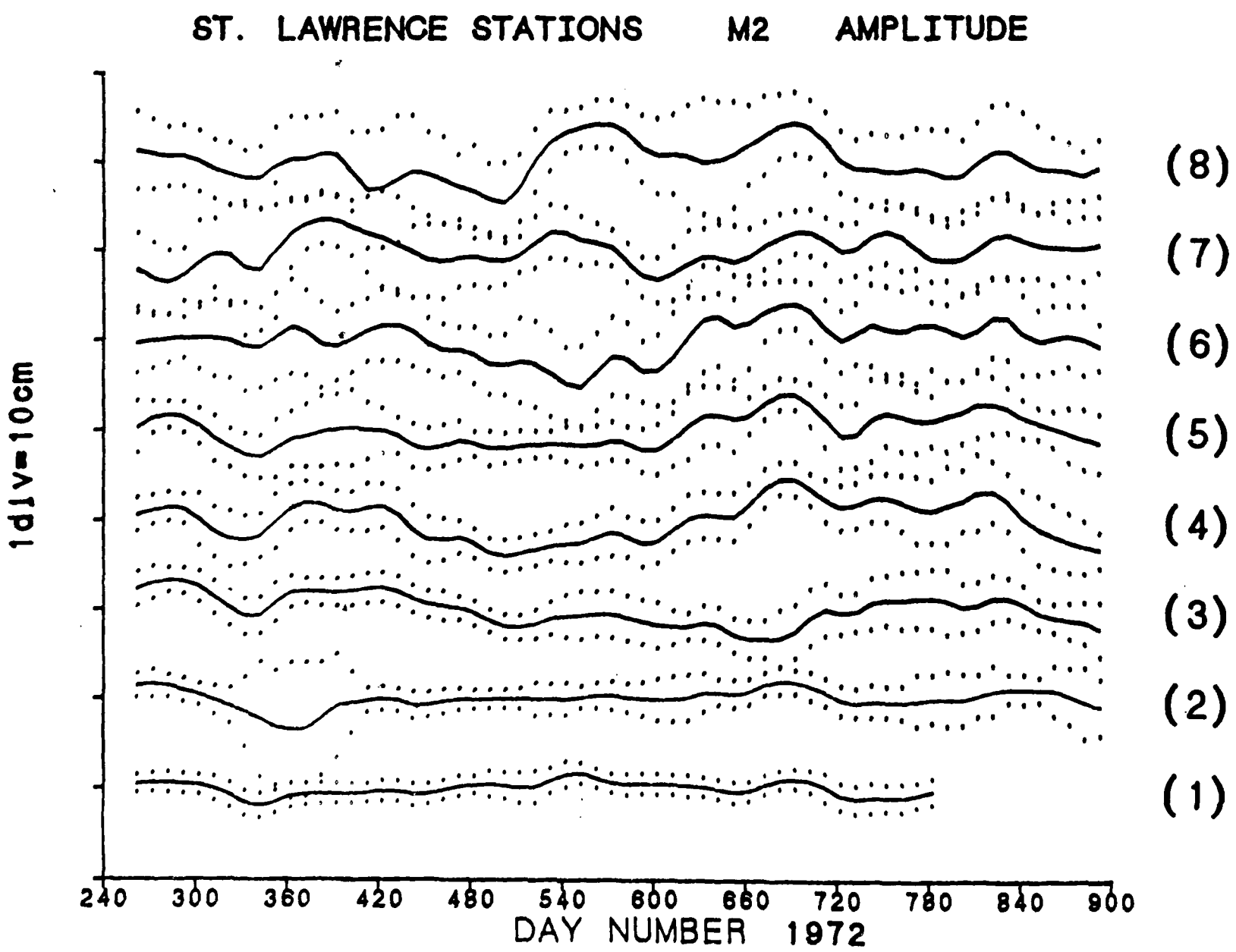
ST. LAWRENCE STATIONS M2 AMPLITUDE
1div=10cm
(8)
(7)
(6)
(5)
(4)
(3)
(2)
(1)
240
300
360
420
480
540
600
660
720
780
840
900
DAY NUMBER 1972

FIGURE 7

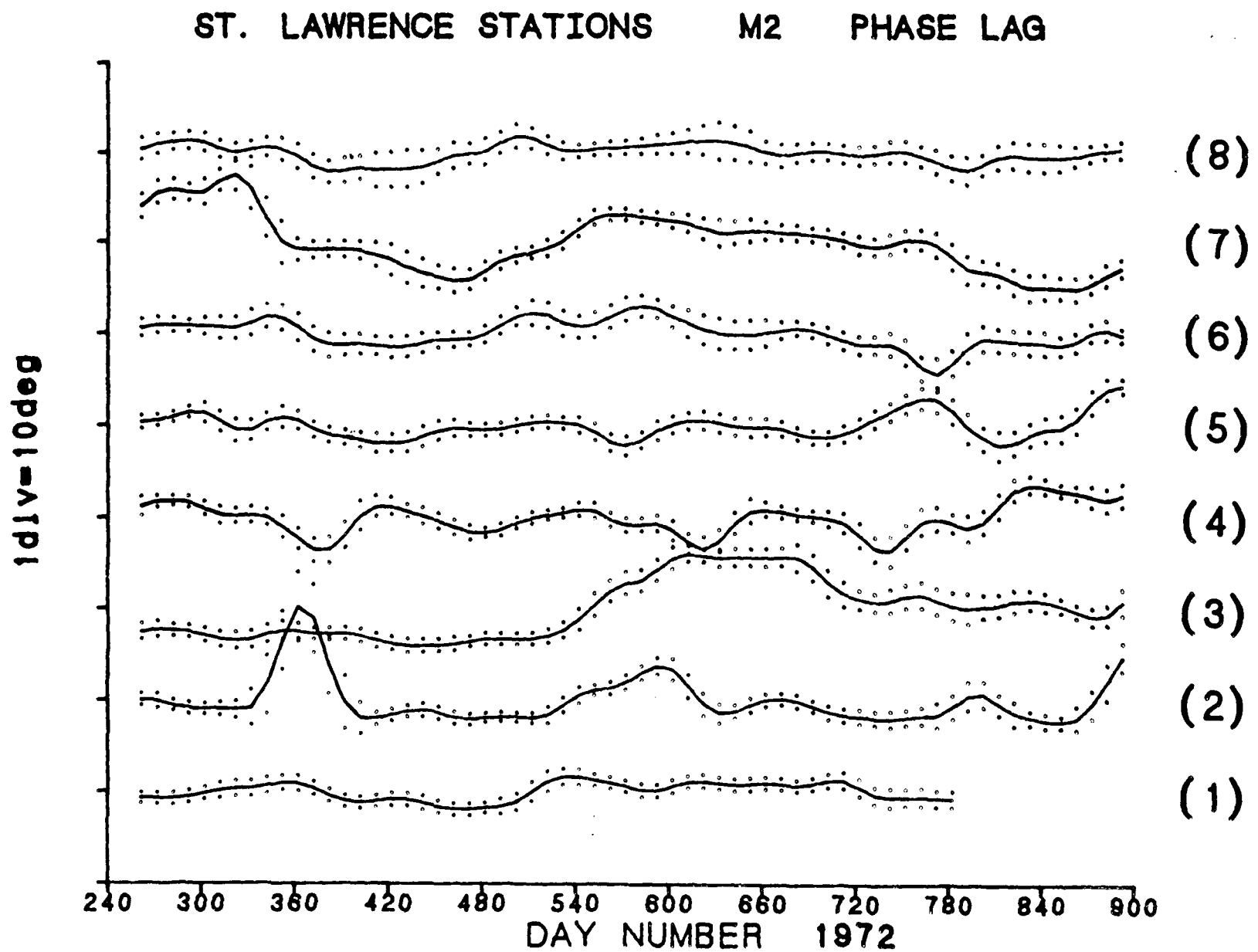
ST. LAWRENCE STATIONS M2 PHASE LAG
1div=10deg
(8)
(7)
(6)
(5)
(4)
(3)
(2)
(1)
240
300
360
420
480
540
600
660
720
780
840
900
DAY NUMBER 1972

FIGURE 8

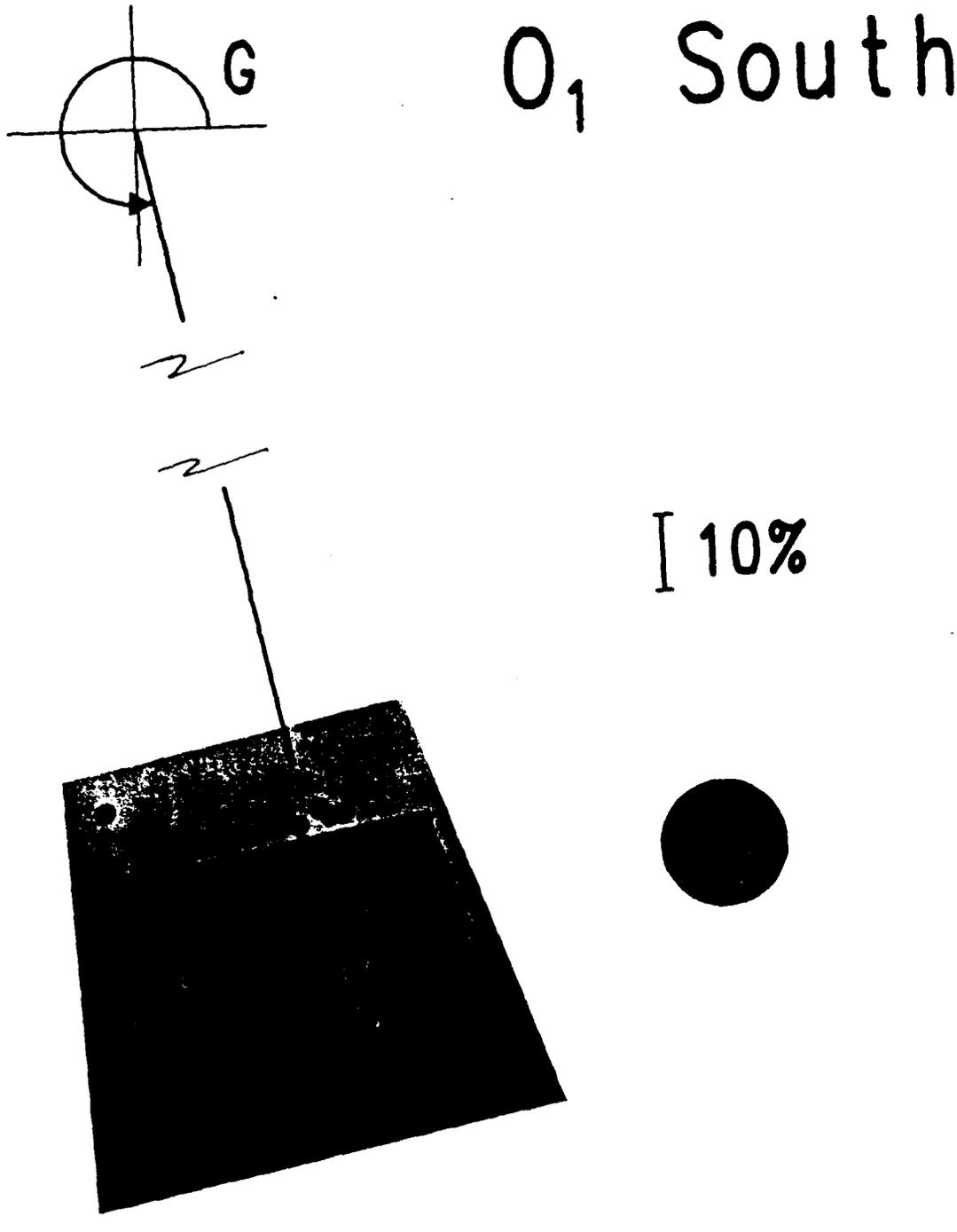

FIGURE 9

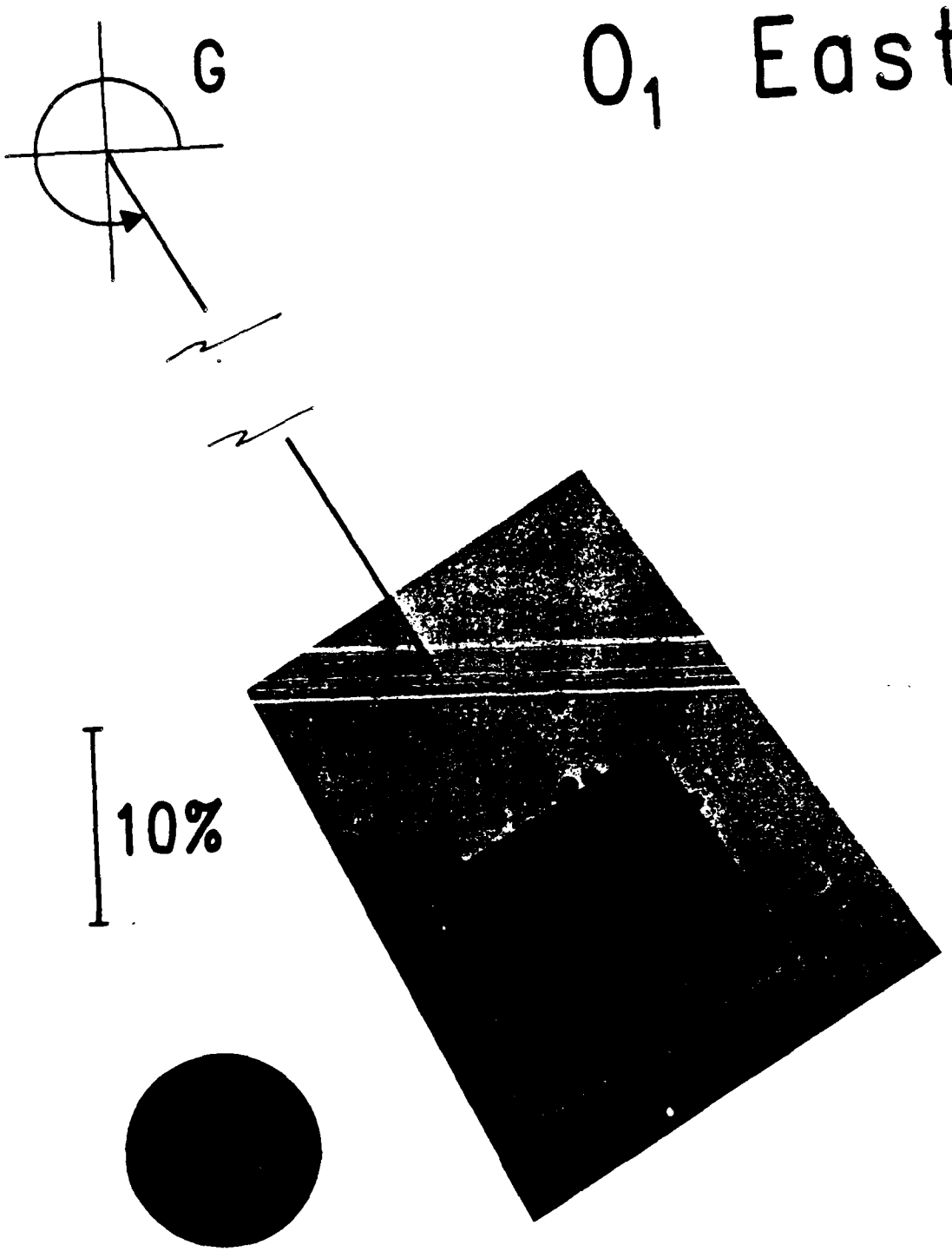

FIGURE 10

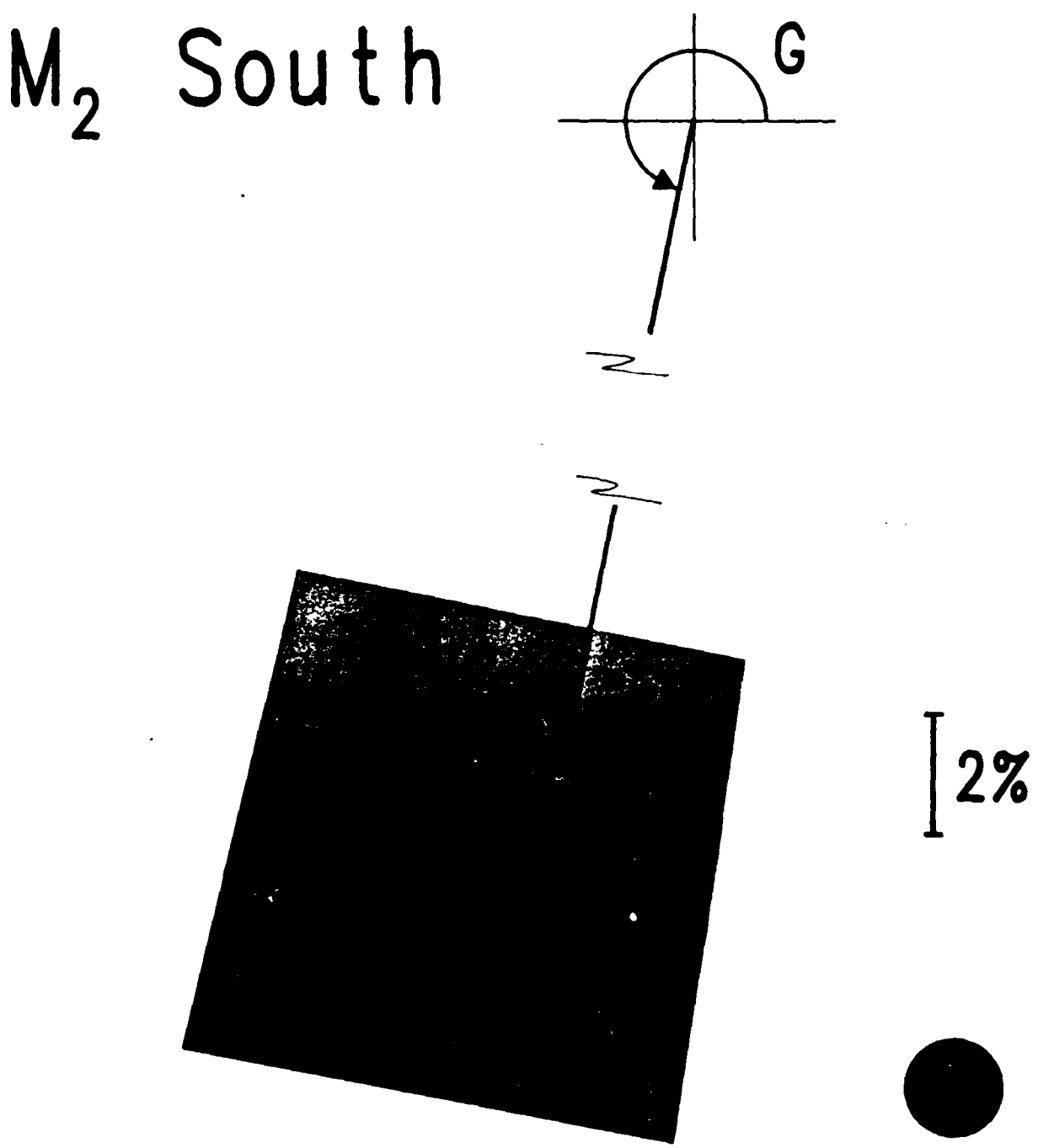

FIGURE 11

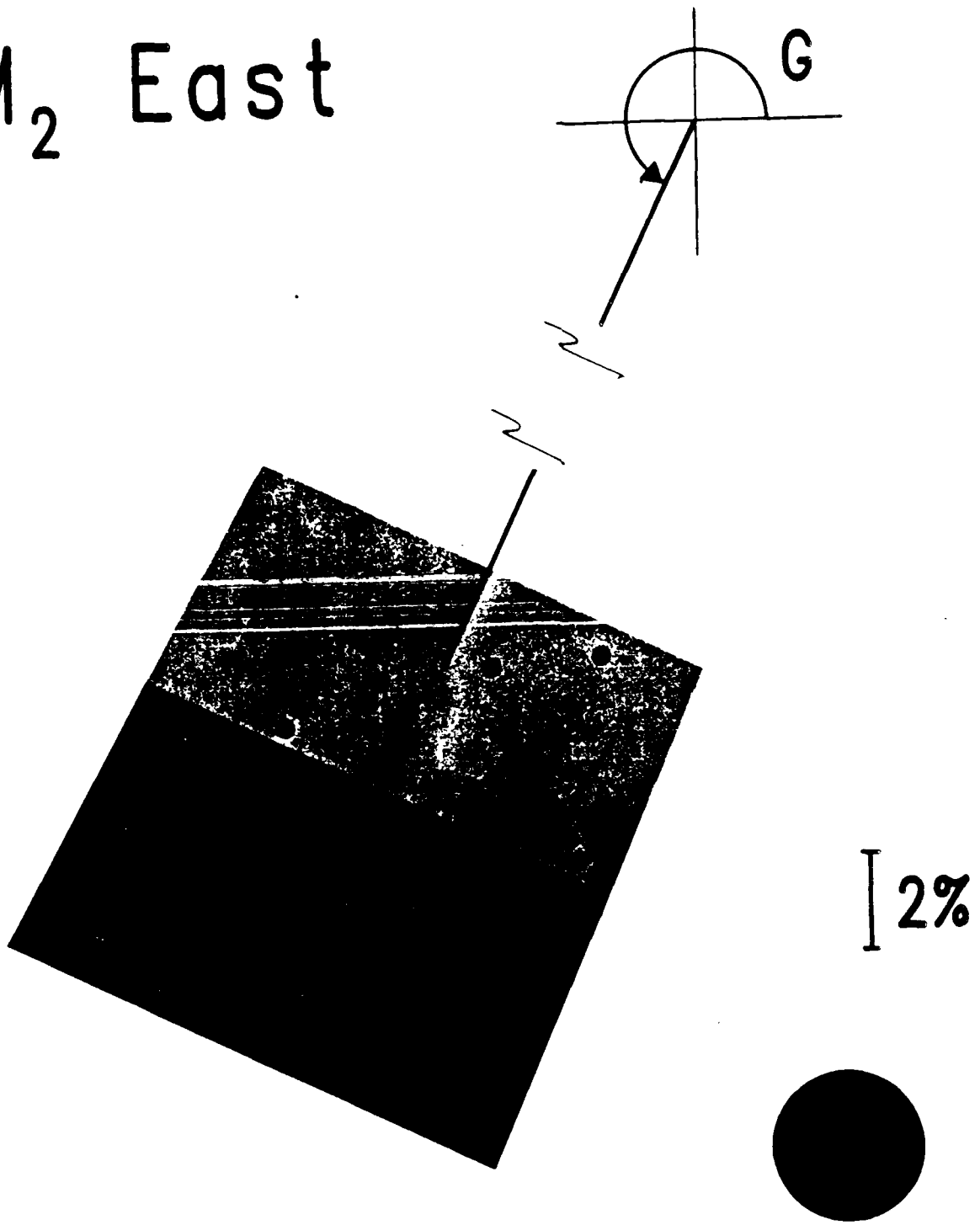

FIGURE 12

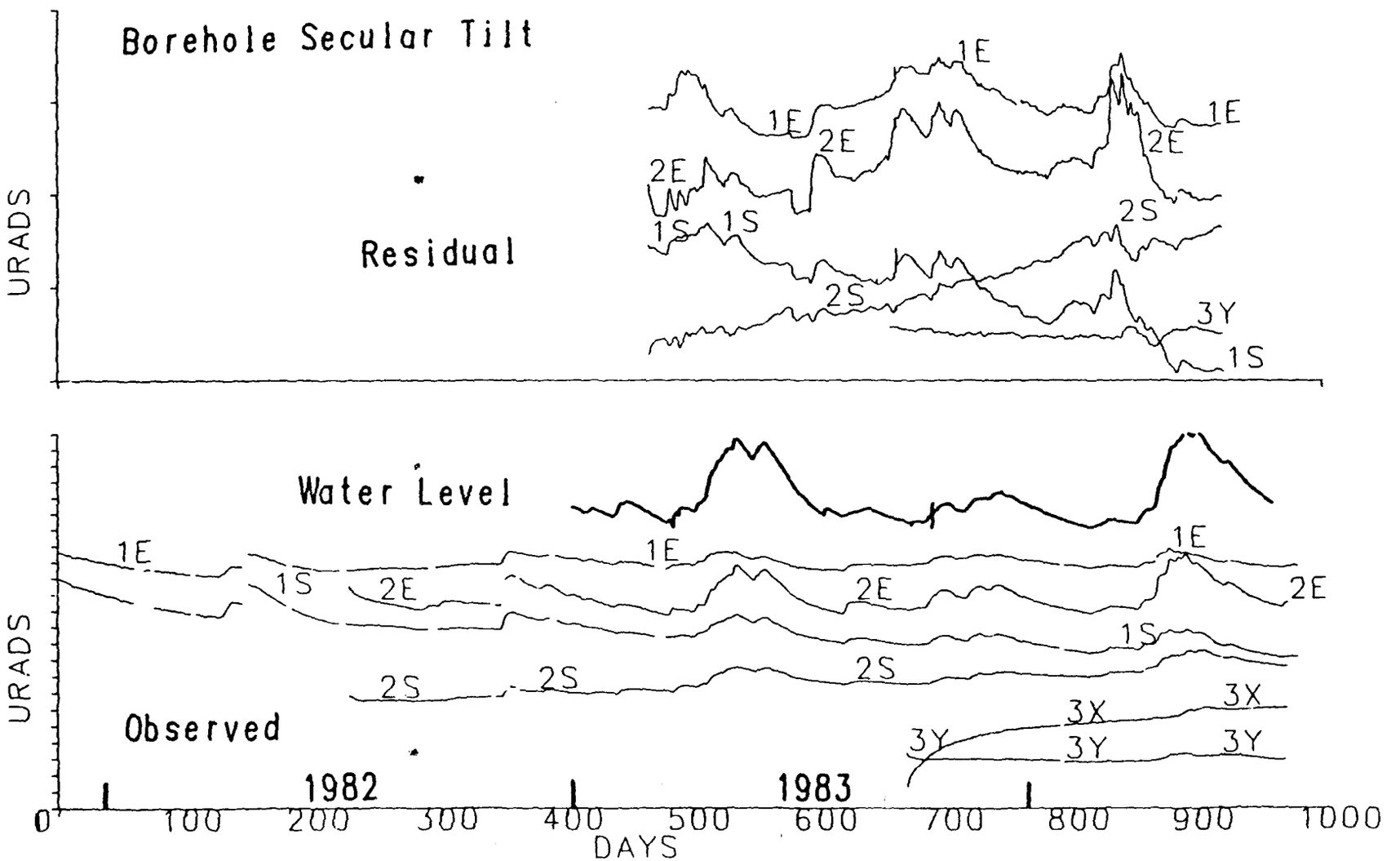
Borehole Secular Tilt
Residual
URADS
1E
2E
1S
2S
3Y
Water Level
Observed
URADS
1E
2E
1S
2S
3X
3Y
1982
1983
0
100
200
300
400
500
600
700
800
900
1000
DAYS

FIGURE 13

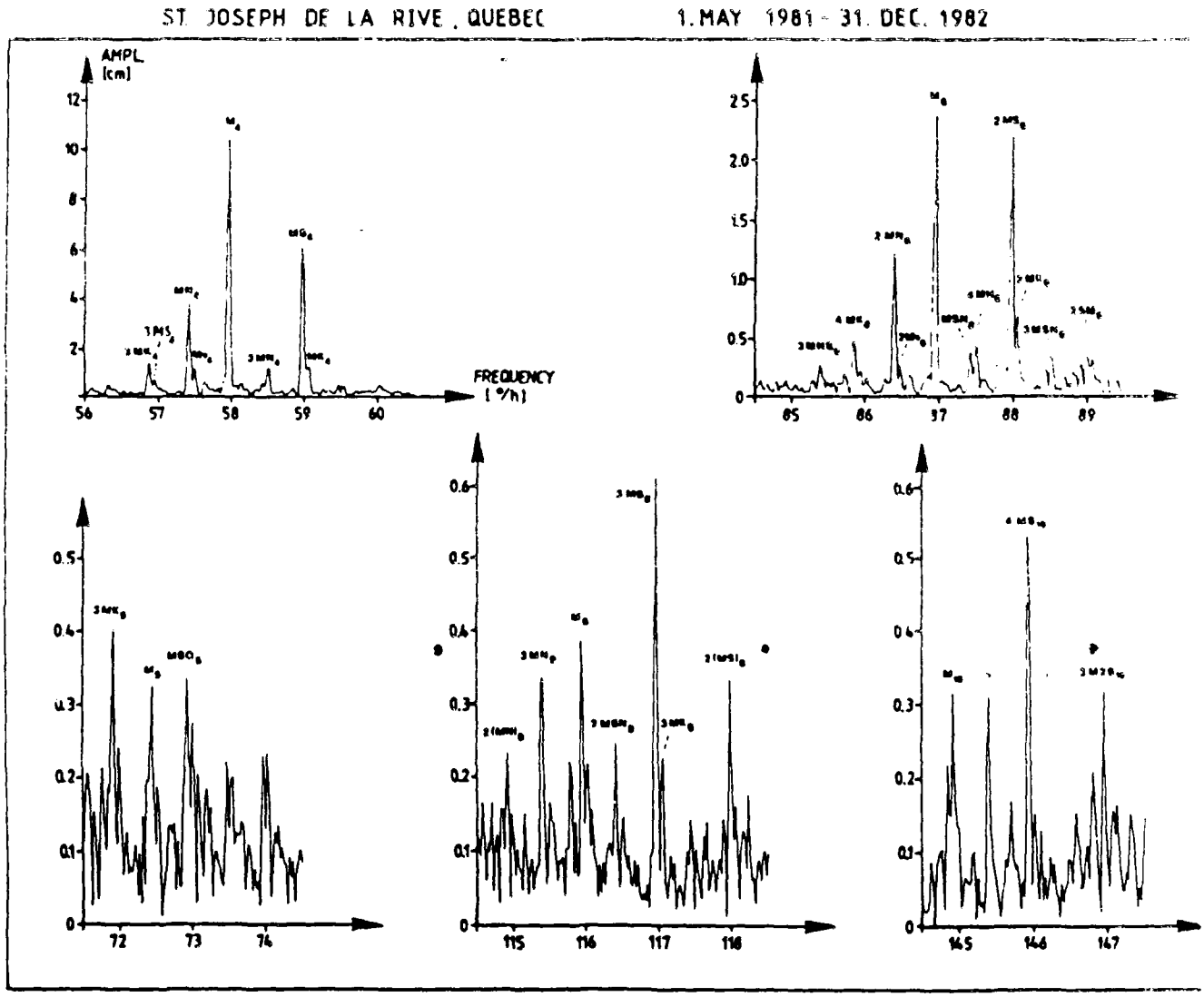
ST. JOSEPH DE LA RIVE, QUEBEC
1. MAY 1981 - 31. DEC. 1982
AMPL
[cm]
FREQUENCY
[°/h]

FIGURE 14